RD&E CENTER

Technical Report

No. 13332

BARRIERLESS ULTRASONIC AIR CLEANER

CONTRACT NO. DAAE07-87-C-R065

JANUARY 1988

B. J. Thomas and S. R. Taylor
S. R. Taylor and Associates
516 SW Kaw
Bartlesville, OK 74003

and

Martin B. Treuhaft
Southwest Research Institute
6220 Culebra Rd.
By San Antonio, TX 78284

U.S. ARMY TANK-AUTOMOTIVE COMMAND
RESEARCH, DEVELOPMENT & ENGINEERING CENTER
Warren, Michigan 48397-5000

NOTICES

This report is not to be construed as an official Department of the Army position.

Mention of any trade names or manufacturers in this report shall not be construed as an official endorsement or approval of such products or companies by the U.S. Government.

Destroy this report when it is no longer needed. Do not return it to the originator.

UNCLASSIFIED

SECURITY CLASSIFICATION OF THIS PAGE

AD-A203 237

REPORT DOCUMENTATION PAGE

Form Approved
OMB No. 0704-0188
Exp. Date: Jun 30, 1986

1a. REPORT SECURITY CLASSIFICATION Unclassified	1b. RESTRICTIVE MARKINGS
2a. SECURITY CLASSIFICATION AUTHORITY	3. DISTRIBUTION/AVAILABILITY OF REPORT Approved for Public Release: Distribution is Unlimited
2b. DECLASSIFICATION/DOWNGRADING SCHEDULE	
4. PERFORMING ORGANIZATION REPORT NUMBER(S)	5. MONITORING ORGANIZATION REPORT NUMBER(S) 13332
6a. NAME OF PERFORMING ORGANIZATION S. R. Taylor and Associates 6b. OFFICE SYMBOL (If applicable)	7a. NAME OF MONITORING ORGANIZATION U.S. Army Tank-Automotive Command
6c. ADDRESS (City, State, and ZIP Code) 516 SW Kaw Bartlesville, OK 74003	7b. ADDRESS (City, State, and ZIP Code) Warren, MI 48397-5000
8a. NAME OF FUNDING/SPONSORING ORGANIZATION U. S. Army Tank-Automotive Command 8b. OFFICE SYMBOL (If applicable) AMSTA-RGT	9. PROCUREMENT INSTRUMENT IDENTIFICATION NUMBER DAAE07-87-C-R065
8c. ADDRESS (City, State, and ZIP Code) Warren, Michigan 48397-5000	10. SOURCE OF FUNDING NUMBERS PROGRAM ELEMENT NO. / PROJECT NO. / TASK NO. / WORK UNIT ACCESSION NO.

11. TITLE (Include Security Classification)
Barrierless Ultrasonic Air Cleaner

12. PERSONAL AUTHOR(S)
Brenda J. Thomas, Scott R. Taylor (S.R.Taylor & Assoc.) and Martin B. Treuhaft (Southwest Res

13a. TYPE OF REPORT	13b. TIME COVERED	14. DATE OF REPORT (Year, Month, Day)	15. PAGE COUNT
Final	FROM _____ TO _____	1988, January	46

16. SUPPLEMENTARY NOTATION

17. COSATI CODES			18. SUBJECT TERMS (Continue on reverse if necessary and identify by block number)
FIELD	GROUP	SUB-GROUP	Ultrasonic, dust, precleaners. (JKS)

19. ABSTRACT (Continue on reverse if necessary and identify by block number)

This report describes an experimental program (SBIR Phase I) to demonstrate the technical feasibility of using an ultrasonic standing wave field to promote coalescence of airborne dusts in order to improve the separation efficiency of typical inertial separators such as current precleaners. Major project tasks included assembly of an ultrasonic coalescence array; measurement of the dust mass passing through an inertial separator as a function of upstream dust concentration, airflow rate, and ultrasonic power level; and calculation of the improvement in separator efficiency as a function of coalescence. The results clearly demonstrate the technical feasibility of using an ultrasonic standing wave field to alter the particle size distribution of airborne dust in order to improve the performance of existing inertial separators, such as those used for precleaners in state-of-the-art air cleaner systems. Importantly, there is no pressure drop across the standing wave field and hence the problems typically associated with barrier filter loading can be avoided.

20. DISTRIBUTION/AVAILABILITY OF ABSTRACT ☒ UNCLASSIFIED/UNLIMITED ☐ SAME AS RPT. ☐ DTIC USERS	21. ABSTRACT SECURITY CLASSIFICATION Unclassified
22a. NAME OF RESPONSIBLE INDIVIDUAL Jack Stevenson	22b. TELEPHONE (Include Area Code) 313/574-6047 22c. OFFICE SYMBOL AMSTA-RGT

DD FORM 1473, 84 MAR 83 APR edition may be used until exhausted.
All other editions are obsolete.

SECURITY CLASSIFICATION OF THIS PAGE
UNCLASSIFIED

TABLE OF CONTENTS

LIST OF TABLES

LIST OF ILLUSTRATIONS

1.0 INTRODUCTION

S. R. Taylor and Associates (SRTA) and Southwest Research Institute (SwRI), acting in a consulting role, are pleased to submit this Final Technical Report describing an investigation of a Barrierless Ultrasonic Air Cleaner funded under U. S. Army Contract No. DAAE07-87-C-R065, a SBIR Phase 1 contract. Major project tasks included assembly of an ultrasonic coalescence array in a bench flow system; measurement of the dust mass passing through an inertial separator as a function of upstream dust concentration, airflow rate, and ultrasonic power level; and calculation of the improvement in separator efficiency as a consequence of ultrasonic coalescence.

Military vehicle air cleaner system performance can be evaluated in several ways, however, one of the most important performance considerations is service life. In fact, it is this parameter that has led to the use of two-stage systems incorporating precleaners. Today, military air cleaners require frequent servicing, particularly when operating in highly dusty environments. In addition to reducing operational readiness, this also poses the particular risks of media contamination and personnel exposure when cleaning must be done in an NBC environment.

This has prompted the Army to seek development of a barrierless air cleaner that would have no moving parts, but which could still maintain a 99.5 % dust removal efficiency with a minimum service life of 50 hours before reaching 20 inches of pressure drop. Essentially, the precleaner operates as such a device in extending the service life of current filters [1,2]. This results because the precleaner removes a large amount of dust that would otherwise have to be handled by the final filter. Since the pressure loss across the precleaner does not increase with time, the overall effect is to slow the pressure drop increase across the filter by lessening its dust burden over time. The improvement in service life, however, is not directly proportional to the performance of the precleaner due to the increase in initial restriction caused by adding the precleaner and the relationship between the new initial restriction, the dust loading rate, and the final allowable restriction. Currently, without a final filter, it is not possible to achieve the desired efficiency.

Ultrasonic vibrations in a standing wave pattern aid separations via ultrasonically enhanced coalescence. While ultrasonic coalescence has been shown to be effective for coalescence of solid and liquid particulates in gaseous fluids and for emulsion separation, the interaction of this phenomena

with other separation/filtration schemes has not been adequately considered.

The theoretical basis for separating a polydispersed suspension of fine solid particles involves the transmission of ultrasonic waves into the bulk fluid, in a standing wave pattern, to cause the smaller particles to collide with the larger particles in order to promote coalescence to a size that is large enough to enable subsequent separation from the bulk fluid. Alternately, ultrasonics can also be used to make two particles of similar size, but different density, coalesce by enhancing a relative velocity between the particles. Importantly, there is no pressure drop across the field and hence the problems typically associated with barrier filter loading can be avoided.

In this project, the effects of an ultrasonic standing wave field on the coalescence of solid particles in a moving airstream were investigated as a function of ultrasonic frequency, power input and duration, and particle size and density. The goal was to determine the feasibility of using ultrasonic coalescence techniques to alter the upstream particle size distribution sufficiently to cause a significant improvement in the separation efficiency of a conventional inertial separator.

2.0 OBJECTIVE

The goal of the Phase I work was to demonstrate the technical feasibility of using an ultrasonic standing wave field to promote coalescence of airborne dusts so as to significantly increase the separation efficiency of an inertial separator by causing the upstream particle size distribution to shift above the separator's nominal cut point as shown in Figure 2-1. In order to meet this goal, the following specific objectives and questions were pursued.

- **Demonstrate the feasibility of transmitting ultrasonic vibrations effectively into a heterogeneous system consisting of air and dust particulate.**
  - Can an ultrasonic standing wave field be produced that will promote rapid coalescence?
  - What are the optimum ultrasonic frequency and power levels required to achieve successful coalescence and size distribution alteration?
  - Can collectors enhance the coalescence of ultrafine particles?

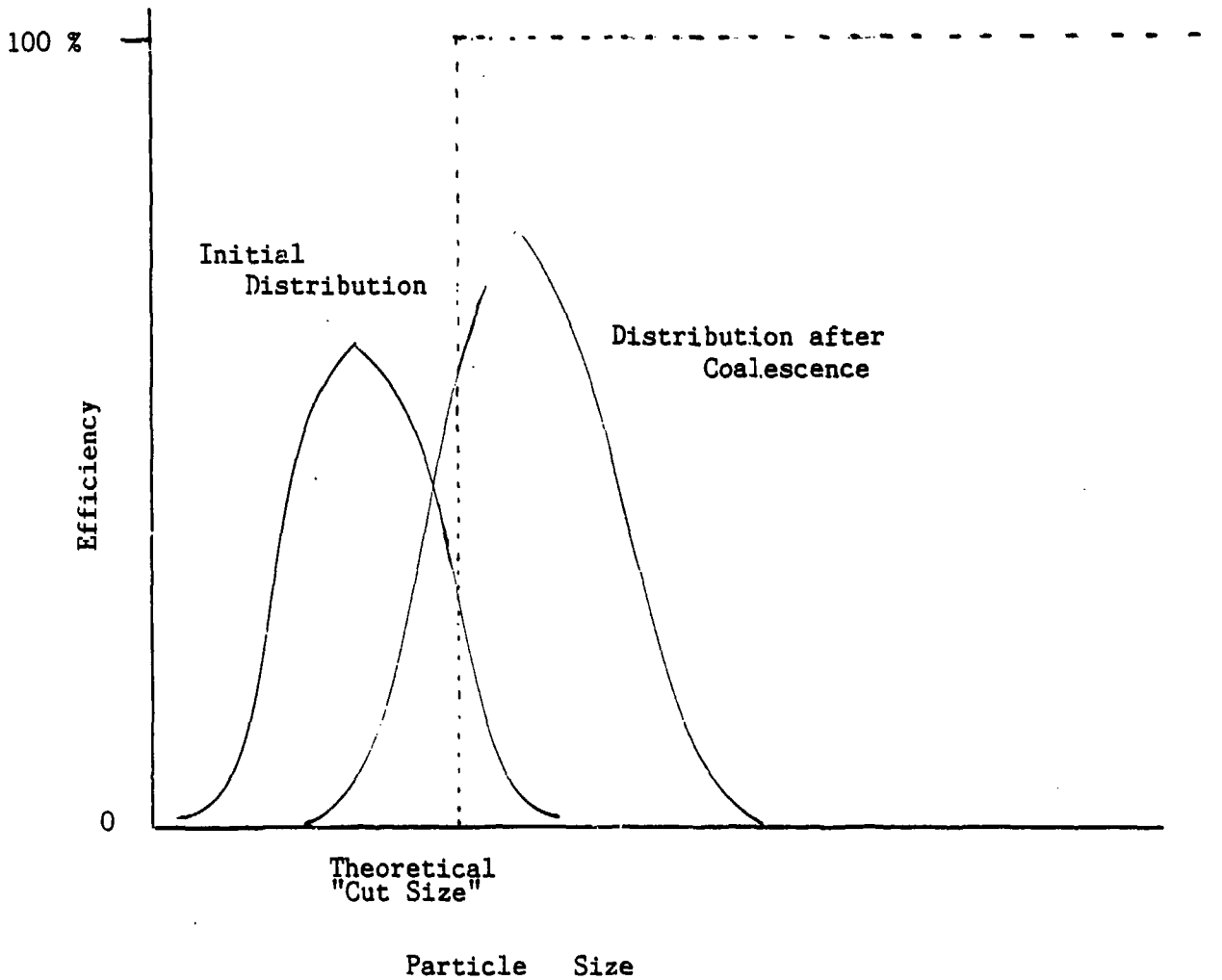

Figure 2-1. Relationship of Separator Efficiency as a Function of the Particle Size Distribution showing the Separator Cut Point

- To what degree does attenuation limit the effectiveness of standing-wave-field-induced coalescence?

- **Demonstrate the feasibility of carrying out continous flow processing.**

  - What are the residence time requirements for successful coalescence in a moving flow field?

  - How do the process variables of temperature and solids content relate to the ability to maintain an effective standing wave field?

  - What variables can be controlled to promote automatic standing wave field operation?

- **Demonstrate the applicability of the process to a variety of feed stream compositions.**

  - How do variations in feed stock composition affect coalescence and separation efficiency?

  - To what degree can variations in feed stock composition be tolerated and how does this relate to systems other than military vehicle air cleaners?

3.0 CONCLUSIONS

Progress to date has been substantial and the technical feasibility of the method has been demonstrated. In particular, the following general conclusions can be made:

- An ultrasonic standing wave field can be generated and maintained under typical dust concentration levels and volumetric flow rates using a specific axisymmetric flexural plate design to provide a unidirectional sound beam.

- Ultrasonic coalescence can increase the particle size distribution of an airborne dust leading to improved separation efficiency in inertial separators typical of existing precleaners.

- The rate of coalescence depends directly on the ultrasonic power input while the degree of

coalescence is directly dependent upon the residence time within the coalescence chamber.

- The rate and degree of ultrasonic coalescence appears to be relatively independent of the dust concentration at least over the concentrations of interest.

- Attenuation of the vibratory energy is dependent upon both the dust concentration and the airflow rate through the coalescence chamber. This limits the chamber pathlength that can be used for ultrasonic coalescence.

- Traditional expressions for the relative motion index appear to be effective for predicting the interaction of the particles with the ultrasonic standing wave field.

- The energy required for coalescence is significantly less in a resonant standing wave field than for a traveling wave field.

The results clearly demonstrate the technical feasibility of using an ultrasonic standing wave field to alter the particle size distribution of airborne dust in order to improve the performance of existing inertial separators, such as those used for precleaners in state-of-the-art air cleaner systems.

Additionally, the effect of variations in the composition of the dust has been shown to have little impact on the coalescence efficiency within the range of interest.

4.0 RECOMMENDATIONS

The feasibility of generating an ultrasonic standing wave field in a flowing airborne dust aerosol has been demonstrated. This is crucial to the Phase II development effort since scale up depends on the ability to maintain a resonant standing wave field over a wide range of dust concentration levels and airflow rates. The results obtained during Phase I point the direction for the Phase II continuous flow work by identifying the critical relationships between the ultrasonic power and chamber residence time requirements.

The Phase II effort should concentrate on (1) scale up of the method to higher airflow rates which are representative of existing equipment, (2) automation of the standing wave field generation and maintenance, and (3) optimization of the inertial separator to take advantage of the coalescence rather

than tailoring the coalescence to fit a particular inertial separator. The results of such an effort will go a long way in assessing the potential for using ultrasonic coalescence as the basis for military vehicle, barrierless air cleaner systems.

5.0 DISCUSSION

5.1 Ultrasonic Equipment Specifications

Ultrasonic vibrations were generated using a Branson Model 102 piezoelectric transducer powered by an ENI EGR-800 power generator having variable frequency (9 - 110 kHz) and power (0 - 800 watts) output capability. Impedance matching of the power generator and the transducers was accomplished with an ENI EVB-1 impedance matching network. The power generator contains a power meter providing a continuous readout of either forward or load power at the generator. Frequency was monitored with a Tenma Model 72-380 frequency counter/function generator. Current and voltage outputs were monitored with a Tenma Model 72-320 dual trace oscilliscope.

5.2 Coalescence Array Design and Assembly

The main coalescence chamber framework and flexural plate were designed to operate at a nominal frequency 20 kHz. The flexural plate was further designed to provide axisymmetric vibrational waves[3], which had previously been shown to be desirable for generating a standing wave field[4-6]. The flow-through array was assembled so that a controlled aerosol could be fed to the inlet of the coalescence chamber. The output of the array was directed to an inertial separator, which was followed by an absolute filter and a suction blower. A schematic of the array is shown in Figure 5-1. In order to investigate a large matrix of flow rates and residence times, the coalescence section was made to accommodate tubes from 4- to 10-inches in diameter and up to six feet in length.

Calibrated flow orifices were used to measure the mainstream flow rate and the scavenge flow from the inertial separator. Blower controls allowed the primary and secondary flows to be controlled during testing. The inertial separator incorporated three axial swirl tubes and was designed to operate at a 10 percent scavenge flow. Figure 5-2 shows a cross-section drawing of one of the swirl tubes wherein it can be seen that passage of the airstream through the initial vanes causes the airstream to rotate about the tube axis thus generating a centrifugal force causing the dust to move to the outer edges of the tube. The position and size of the output tube controls the cutoff size. Prior to use, performance, in terms of pressure drop and efficiency, was measured at SwRI using AC

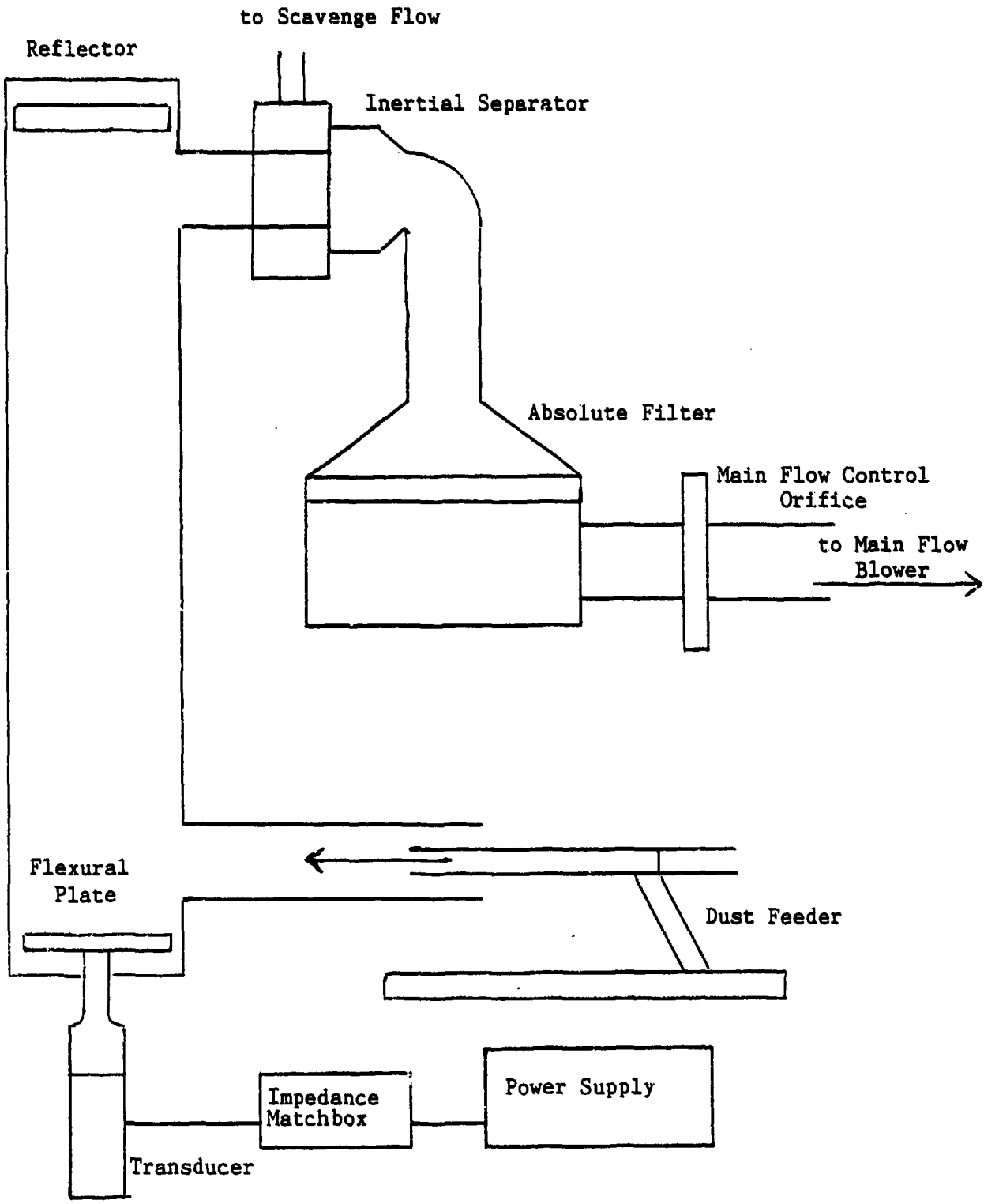

Figure 5-1. Schematic of the Ultrasonic Coalescence Flow Array

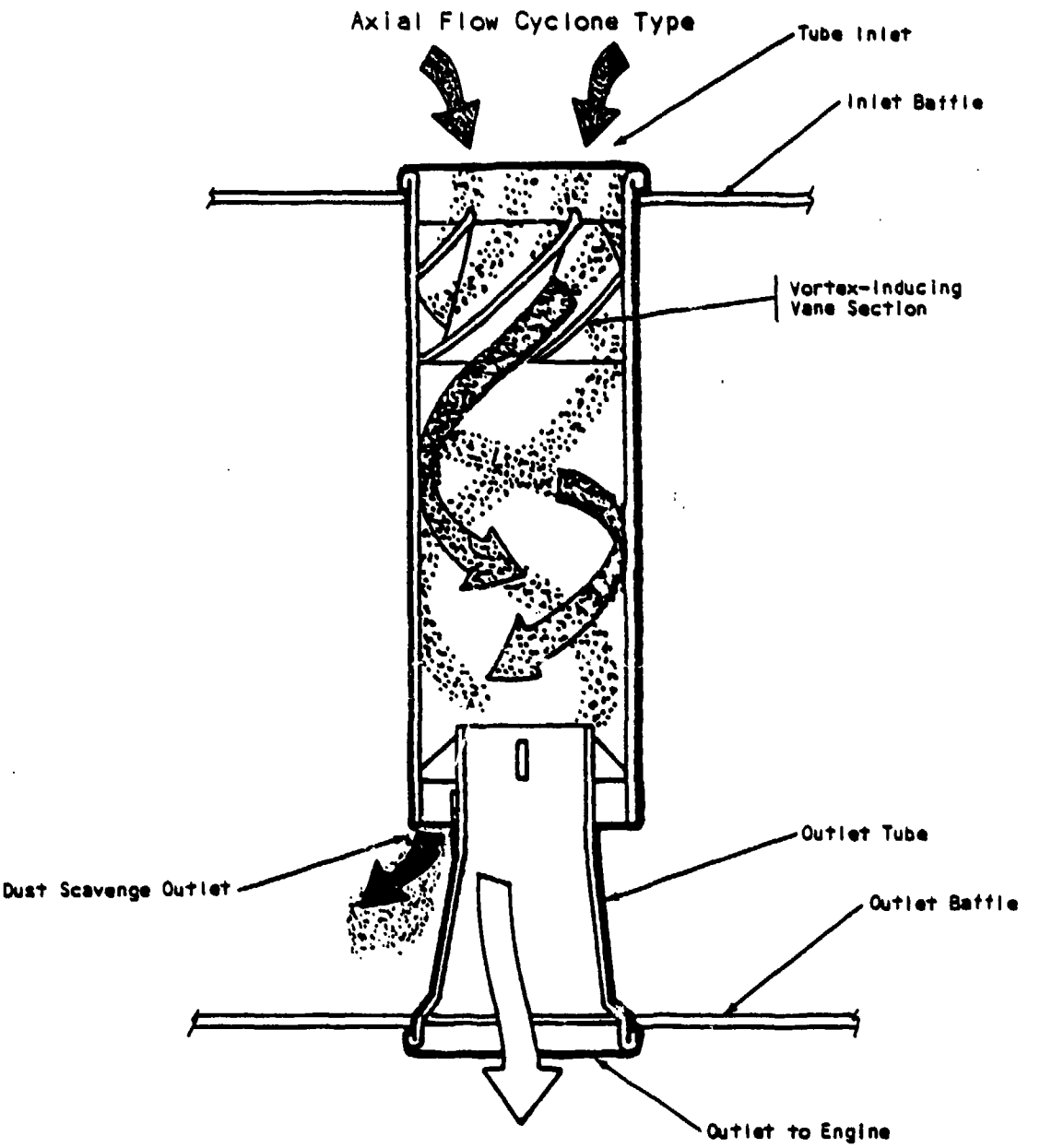

Figure 5-2. Cross-section Drawing of a Typical Swirl Tube Inertial Separator

Fine and Coarse test dusts. The separator was sized to have a moderate efficiency on these dusts, the original thinking being that coalescence would cause a significant improvement from these levels. Figure 5-3 shows a photograph of the complete flow array, with a 10-inch-diameter coalescence tube.

While the main flow array was being fabricated and assembled, several tests were conducted using an existing 4.5-inch-diameter coalescence array. This array could accommodate chamber lengths up to two feet. The flexural plates were of the axisymmetric design and operated at 23.2 and 27.1 kHz.

5.3 Dust Materials

AC Coarse and Fine test dusts were chosen for use on the project and these were obtained from AC Spark Plug Division of General Motors Corporation. While awaiting delivery of the AC dust, a clay material was used for some of the initial tests. Table 5-1 gives the particle size distributions of the AC and clay dust materials. Figure 5-4 shows the baseline efficiency of the inertial separator with respect to each of these dusts.

5.4 Parametric Analysis

Two theories have been developed which treat the covibration of suspended particles in a fluid medium. The relative motion, R, between the particle and the medium, due to ultrasonic vibration, is a convenient means of expressing the phenomenon. The Brandt, Freund and Hiedemann derivation for relative motion[7] leads to nearly the same mathematical expression given in later work by St. Clair[8]. The Hiedemann form is:

$$R = \frac{X_p}{X_m} = \frac{1}{\left\{1 + \left(\frac{\pi d^2 f(\rho_p - \rho_m)}{9\eta}\right)^2\right\}^{\frac{1}{2}}}$$

where

X_p, X_m = amplitudes of motion of particles and medium, respectively (cm),

d = particle diameter (cm),

f = frequency (Hz),

Figure 5-3. Photograph of the Vertical Simulated Air Cleaner Array

Table 5-1. Test Dust Particle Size Distribution By Weight, %

Size, microns	Clay	Coarse	Fine
0 - 5	25	12 ± 2	39 ± 2
5 - 10	29	12 ± 3	18 ± 3
10 - 20	31	14 ± 3	16 ± 3
20 - 40	13	23 ± 3	18 ± 3
40 - 80	2	30 ± 3	9 ± 3
80 - 200	---	9 ± 3	---

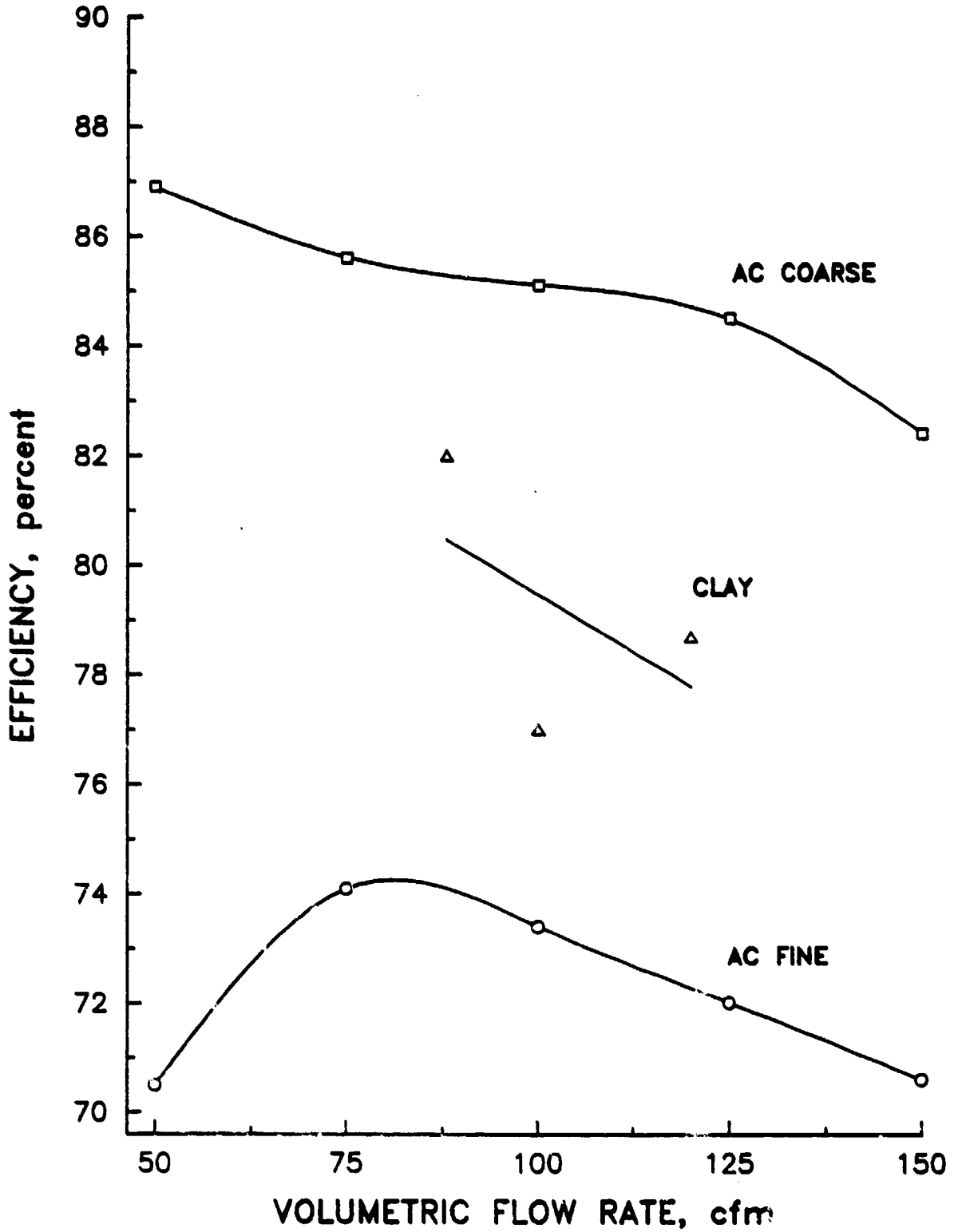

Figure 5-4. Baseline Efficiency of the Three-Tube Separator at 10 % Scavenge. The Upstream Dust Concentration was 0.025 grams per cubic foot air

ρ_p, ρ_m = densities of paticle and medium, respectively (g/cc), and

η = viscosity of the medium, poise (g/cm/sec).

When the medium is a gas, $(\rho_p - \rho_m)$ is not significantly different in value from ρ_p and Hiedemann's equation reduces to St. Clair's.

Calculations were made to show the effect of variations in frequency and particle density on the relative motion index according to the Hiedemann expression. Figure 5-5 shows the results of these calculations. It can be seen that the particle size at which $R = 0.5$ is indirectly proportional to the frequency and that the frequency needs to be above 10 kHz in order to achieve a relative motion difference between particulate smaller than 2 microns and the bulk fluid.

During the course of the initial literature search for pertinent work in this field, contact was made with Dr. Gerhard Reethof, Director of the Noise Control Laboratory at Pennsylvania State University. Dr. Reethof is actively investigating the accustic agglomeration of fly ash and has published several recent papers[9-12] on theoretical aspects and modeling, including the description of a computer model to predict variation in an aerosol size as a function of the process variables. Initially, it was thought that this model could be used to predict inertial separator performance as a function of the coalescence process variables. Unfortunately, one of the key assumptions in the model is that the vibrations are in the form of a traveling wave, which differs from the current work where a well-defined standing wave field was maintained. Work to date has shown significant coalescence in standing wave fields with sound pressure levels on the order of 120 dB, well below the levels of 140-160 dB used by Reethof et al. in order to achieve significant rates of agglomeration.

Additionally, their models are based on the use of much lower frequencies in order to alleviate attenuation effects. We believe that attenuation will be much less of a problem in a resonant standing wave field since high initial sound pressure levels should not be required to achieve significant rates of coalescence.

Finally, their work indicates that successful coalescence required treatment times of 2-6 seconds. If these times cannot be shortened, equipment for realistic treatment volumes will be much too large for vehicle applications. It is our belief that these times can be significantly shortened through by using a

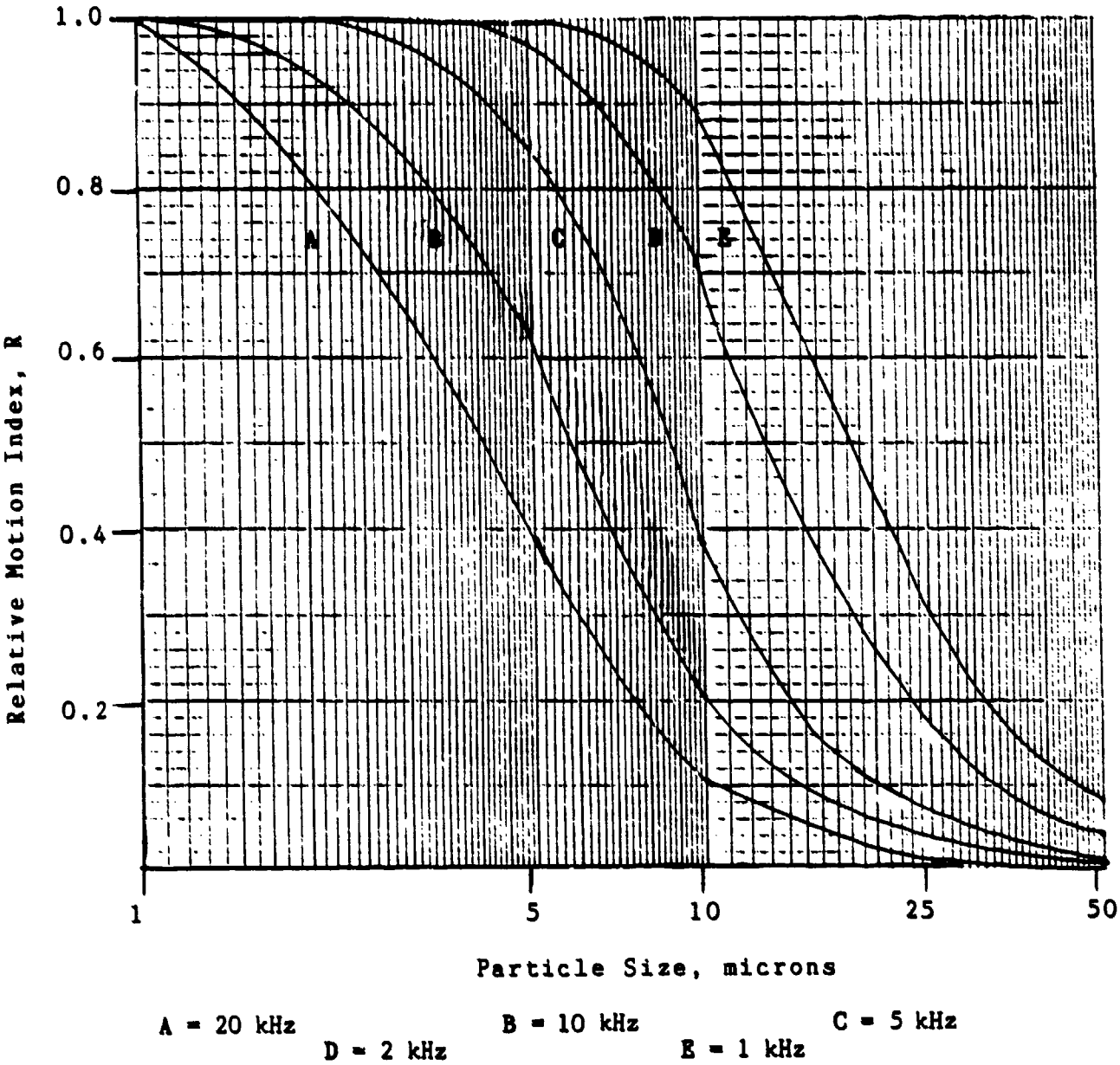

Figure 5-5. Relative Motion Index as a Function of Frequency

standing wave field which will maximize the energy transfered into the aerosol.

5.5 Initial Parametric Testing

While work to fabricate and assemble the complete bench flow array was underway, some initial experiments were conducted to evaluate the basic coalescence idea. In these experiments, the 4.5-inch-diameter array was used as both a coalescence chamber and as a crude inertial separator. Since the chamber orientation was horizontal, inertial fallout within the chamber depended on the characteristics of the dust and the airflow rate through the chamber. Figure 5-6 is a photograph of the coalescence chamber taken after an ultrasonic test; particle fallout, as evidenced by the dust collected at the nodal points in the standing wave pattern, is clearly visible.

In order to develop quantitative data, known amounts of the test dust were fed through the array and into a filter trap, which was then weighed to determine the amount of material that penetrated the chamber. The experiment was repeated with the flexural plate activated at 27.1 kHz with an input power of 25 watts. Two different positions of the reflecting plate were tried; in position A, the reflector plate was 1/8 inch from the back of the chamber while position B had the reflector plate at the back of the chamber. The data in Table 5-2 show that nearly twice as much material was captured in the tube when the ultrasonics were on.

Additional tests were conducted during which the ultrasonic power input, residence time and dust concentration were varied. The data, presented in Figures 5-7 and 5-8, show that qualitatively, coalescence depends directly on the ultrasonic power input and residence time. The airflow during these tests was on the order of 25-30 cfm.

5.6 Continuous Flow Tests

After assembly of the full array, checkout tests were conducted to verify proper operation of the equipment. Additionally, tests were conducted to calibrate the three-tube separator with the clay that was used in some of the earlier test work.

In order to evaluate the ability of the flexural plate to develop a unidirectional sound beam, the sound pressure was mapped in the following manner. A sound pressure meter was positioned 5 feet from the flexural plate and then moved to several positions off the central axis to map sound pressure as a function of lateral position. Figure 5-9 shows the results

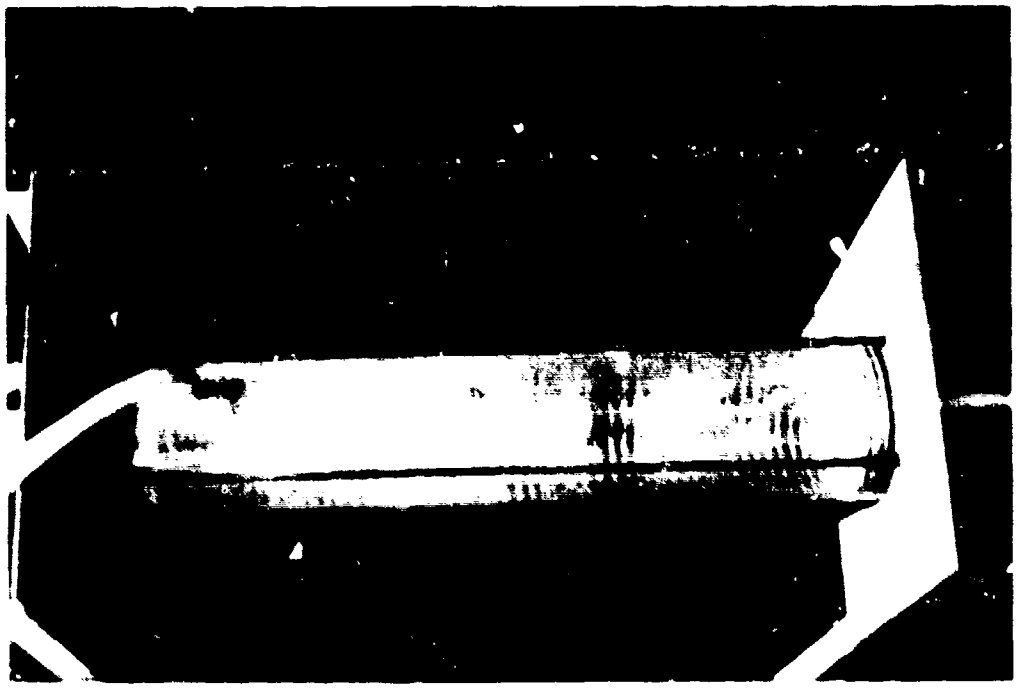

Figure 5-6. Photograph of the 4.5-inch Coalescence Array showing Dust Fallout at the Standing Wave Field Nodal Planes

Table 5-2. Ultrasonic Coalescence Tests

Dust Fed	Time	Dust Trapped	Efficiency	Ultrasonics
10	3:06	8.86	11.4	NO
10	4:05	7.90	21.0	NO
10	3:58	5.43	45.7	NO
10	3:50	6.10	39.0	NO
10	3:24	3.67	63.3	NO
AVERAGE		6.40	36.0	
10	3:11	3.48	65.2	Position A
7.7	3:27	3.23	67.7	"
10	2:30	3.14	68.6	"
10	3:05	3.80	62.0	"
10	3:26	4.40	56.0	"
AVERAGE		3.61	63.9	
10	2:00	3.54	64.6	Position B
10	3:01	4.11	58.9	"
10	2:10	3.42	65.8	"
10	2:52	3.83	61.7	"
10	3:21	4.15	58.5	"
AVERAGE		3.81	61.9	

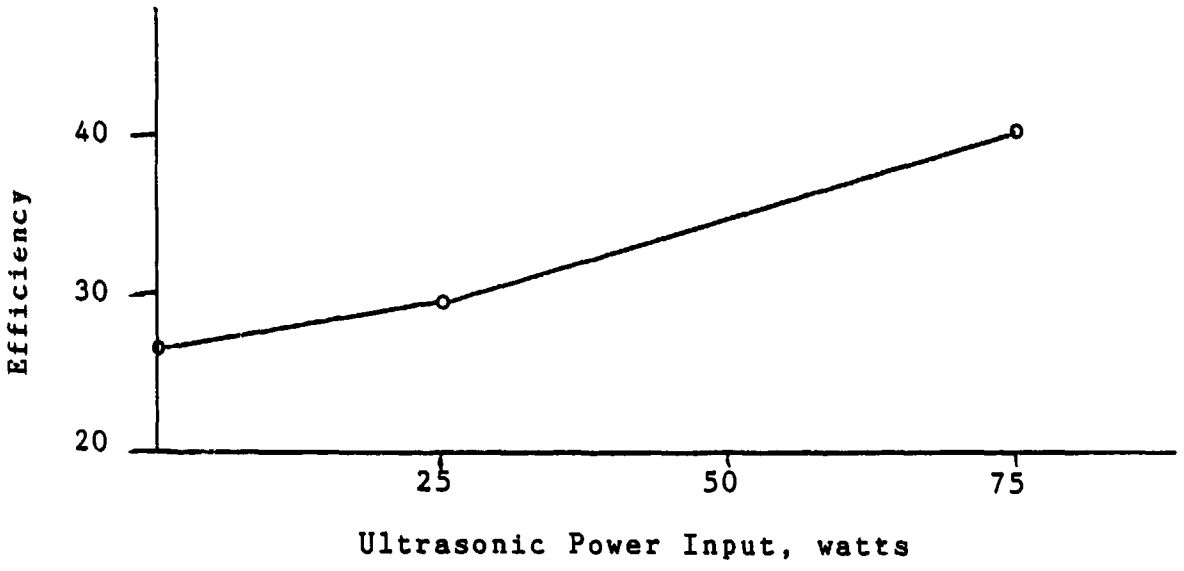

Figure 5-7. Parametric Evaluation of the Effect of Ultrasonic Power Input on Coalescence Efficiency

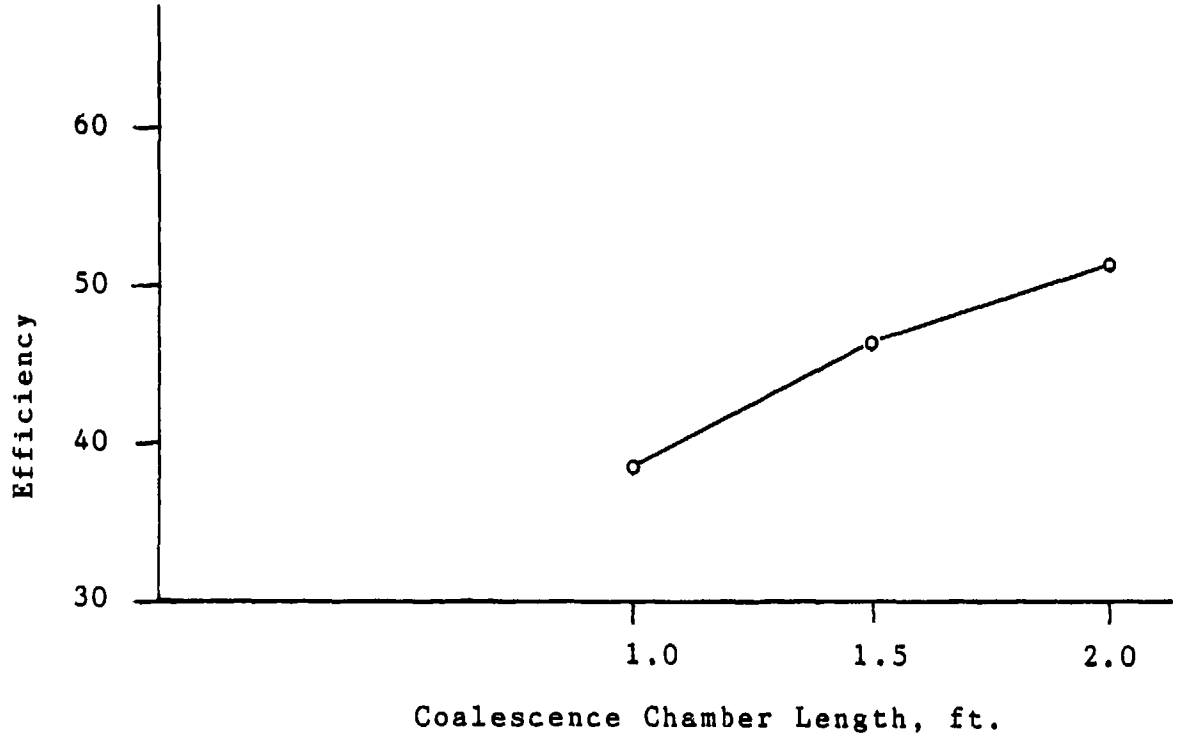

Figure 5-8. Parametric Evaluation of the Effect of Standing Wave Field Length (Residence Time) on Coalescence Efficiency

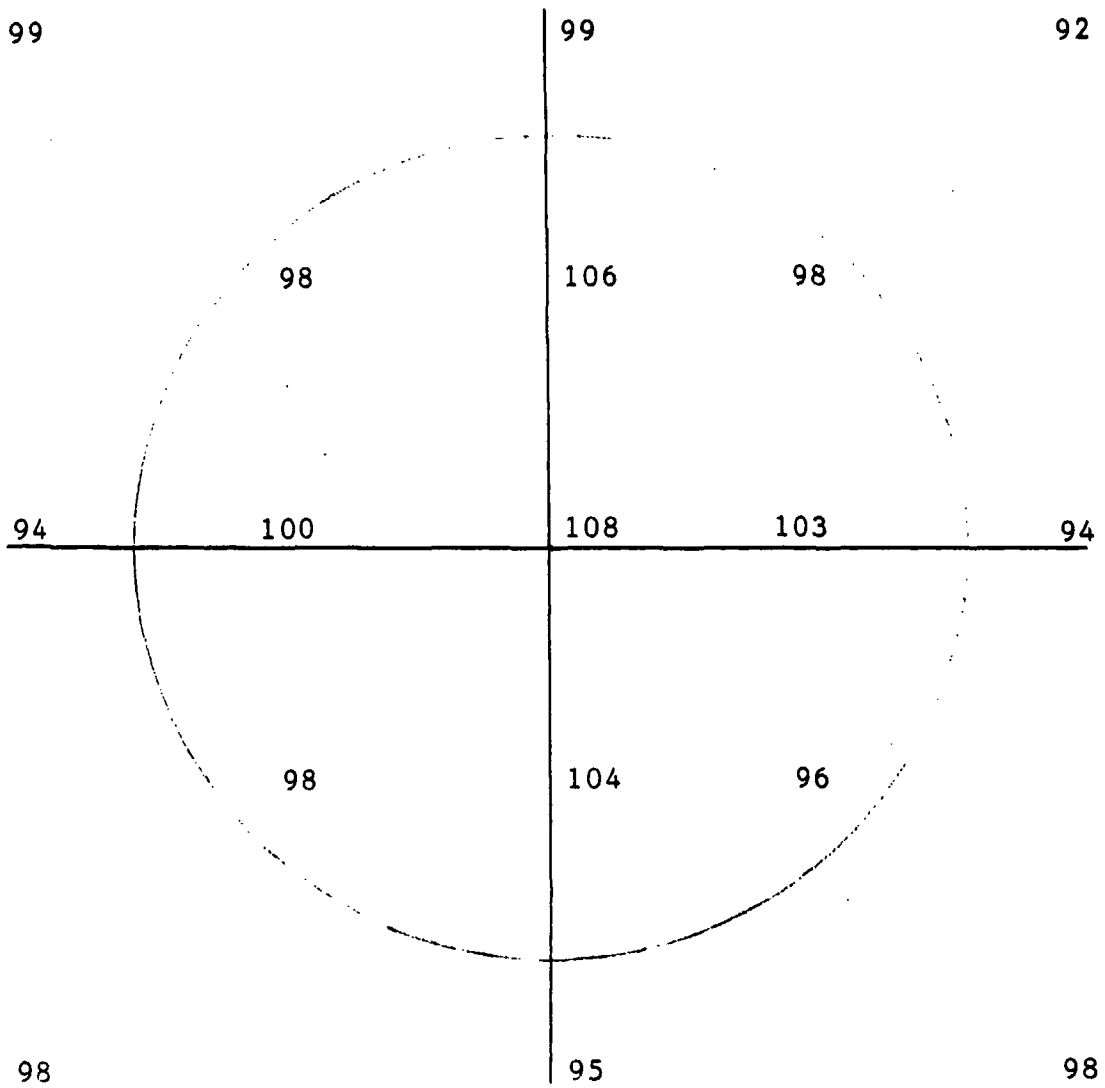

Figure 5-9. Coalescence Chamber Sound Pressure Measurement as a Function of Distance off the Primary Longitudinal Vibrational Axis (dB)

of this mapping for several different ultrasonic power levels. As can be seen, the beam is highly directional and well centered about the axis of the plate. This will allow for accurate dimensional tuning in order to optimize the standing wave field and may also provide a means to automatically tune the standing wave field by monitoring the resonant condition at the reflector plate.

Initial checkout testing to assure correct operation of the inertial separator and all flow measuring equipment was conducted. For the most part, these tests were conducted without any optimization of the ultrasonic standing wave field and with simple, manual dust feeding, which was primarily intended to test operational capability and to aid in working out a proper test procedure. Nevertheless, the results demonstrated an improvement in inertial separation under ultrasonic treatment, as shown in Table 5-3.

5.7 Simulated Air Cleaner Tests

After the initial checkout testing, it was felt that a vertical orientation of the coalescence chamber might provide even greater dust agglomeration and the array was modified to allow this orientation. Continuous flow tests were then conducted, using AC Coarse and Fine dusts, to evaluate the effect of the ultrasonic coalescence on the performance of the inertial separator. Results of these tests are shown graphically in Figure 5-10, where separator performance is shown with and without ultrasonic enhancement. Clearly, there is a significant improvement in the separator efficiency when the ultrasonics are used to enhance coalescence. Furthermore, this improvement does not appear to be particularly sensitive to variation in the dust concentration over the range of interest.

Tests also were conducted with the coalescence chamber in place, but without ultrasonic activation; to provide a control in the nonultrasonic case. Results for these tests are included in Table 5-4. At first, these results were confusing because they suggested that the ultrasonic standing wave field, which was clearly seen to be interacting with the airborne dust, was not altering the size distribution sufficiently to enhance separator efficiency. However, upon closer examination, it became obvious that this apparent contradiction was a result of the particular separator used for these Phase I studies and of the experimental conditions selected.

Initially, it was felt that the most dramatic results, that is, the largest increase in separator efficiency, would be obtained by using an inertial separator that had a fairly low, baseline efficiency. As it turned out, however, a separator having a

Table 5-3. Three-tube Separator Efficiency with Ultrasonic Coalescence

Airflow, cfm	Scavenge, cfm	Dust Conc., gm/ft	Ultrasonic Power, watts	Efficiency*
100	10.0	0.025	0	77†
107	10.8	0.065	0	81.57
102	10.3	0.072	0	79.94
107	10.8	0.063	125	84.78
106	9.8	0.067	125	83.74

*Efficiency = 100 * (Dust Fed - Absolute Filter wt. gain)/ Dust Fed

†Baseline Separator Performance

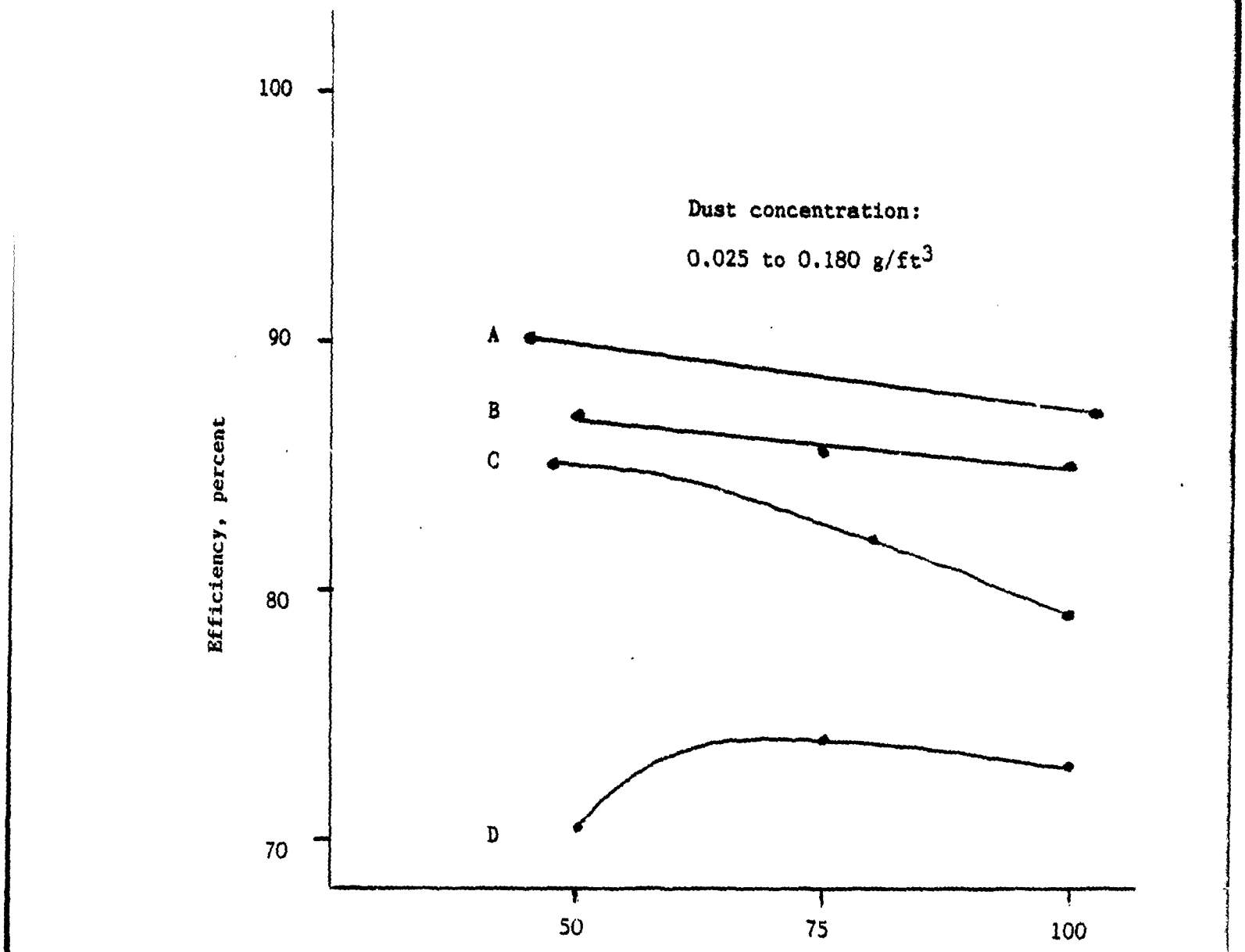

A - AC Coarse, with ultrasonics
B - AC Coarse, without ultrasonics
C - AC Fine, with ultrasonics
D - AC Fine, without ultrasonics

Figure 5-10. Performance of the Three-Tube Inertial Separator with and without Ultrasonic Enhancement during Simulated Air Cleaner Tests

Table 5-4. Simulated Air Cleaner Efficiencies

Airflow, cfm	Scavenge, cfm	Dust Conc., gm/ft^3	Ultrasonic Power, watts	Efficiency*
100	10.0	0.025c	0	86†
100	10.0	0.025f	0	73†
110	10.0	0.108c	0	91
110	10.0	0.080c	85	87
47	4.3	0.19c	0	91
47	4.3	0.18c	50	90
47	4.3	0.194f	0	86
47	4.3	0.178f	50	85
81	7.4	0.161f	0	85
77	6.9	0.132f	100	82

*Efficiency = 100 * (Dust Fed - Absolute Filter wt. gain)/ Dust Fed

†Baseline Separator Performance

c=AC coarse; f=AC fine

lower cut point would have been a better choice. The results in Table 5-4 show that, even though the standing wave field was interacting with the dust (visual observation), coalescence did not shift the particle size distribution far enough toward the cut point to improve the separator's overall efficiency. Had a higher efficiency separator been used, however, the cut point would have been lower, and it is likely for this case that the particle size shift would have been sufficient to cause a meaningful improvement. In other words, although ultrasonic enhancement likely increased the average size of the particles at the lower end of the distribution, it did not increase their size above the cut point of the low efficiency separator and consequently they were still not removed by the separator.

Figure 5-11 shows particle size distribution curves for AC Coarse and Fine test dusts and indicates that the separator's cut point for these dusts should be at the 4 to 5 um level. Figure 5-11 also shows a curve for the relative motion index at 20 kHz as a function of particle size. This curve, which shows (at this frequency) a high degree of relative motion for particles that are well below the cut size, and the particle size distribution curves with their cut points, suggest that it would be possible to significantly alter the size ditribution of the unagglomerated dust without dramatically increasing the percentage of material above the separator's cut point (for this particular, low efficiency separator).

A comparison of the results from tests with fine and coarse supports this contention. As can be seen from Figure 5-10, more improvement occured with the fine dust than with the coarse dust, which had considerably less material below 5 um, nd therefore, considerably less interaction with the standing ave field.

ditionally, it was visually observed that a considerable portion of the dust fed during the nonultrasonic tests simply fell out in the coalescence chamber and, hence, didn't reach the separator. In other words, the total amount of dust presented to the separator was different depending on whether the test was ultrasonic or nonultrasonic. Since only the dust collected on the absolute filter could be determined during these tests, any variation due to fallout in the coalescence chamber itself would not be reflected in the resulting efficiency calculations. Obviously, if less material was presented to the separator during nonultrasonic tests, tne actual separator efficiency was considerably poorer than that calculated from the absolute filter weight alone.

All of these results strongly indicate that ultrasonic enhancement will be more successful when applied in conjunction with the higher efficiency separators. This is very

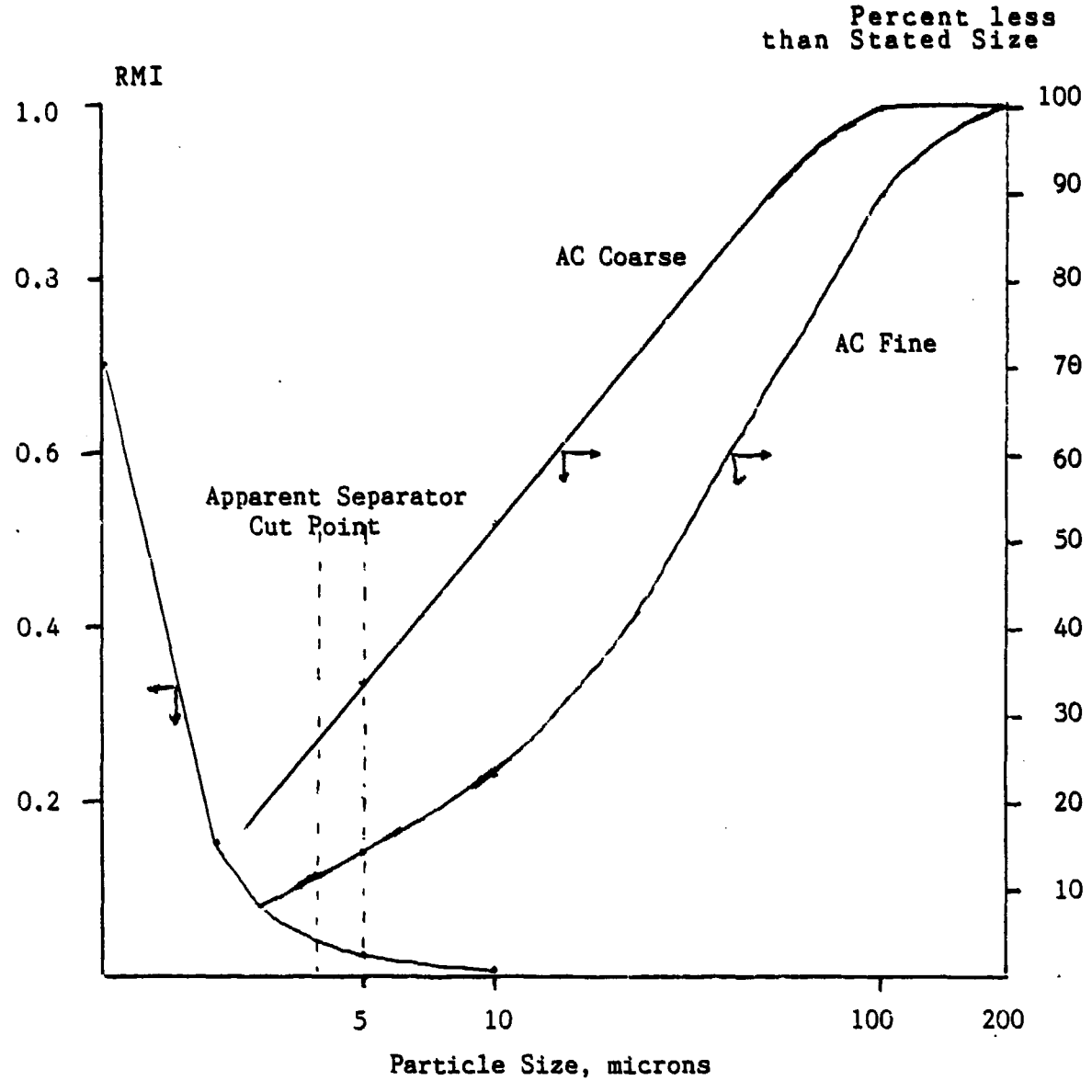

Figure 5-11. Test Dust Size Distribution versus Apparent Separator Cut Point and Relative Motion Index

encouraging because it means one should be able to boost efficiency at the high end which is necessary for a barrierless air cleaner. The data clearly shows that there is a better chance for improving the efficiency of say a 93-95 % separator to a meaningful level than there is of boosting the efficiency of a 85 % separator to the same level. It is recommended that testing with higher efficiency separators be accomplished.

In order to estimate the minimum required residence time for successful coalescence, the absolute filter was removed from the flow array thus allowing flow rates of up to 160 cfm. AC fine dust was fed to the coalescence chamber and the chamber was monitored visually for evidence of standing waves. Since the standing wave pattern was visible at the highest possble flow rate, this represents the shortest residence time achievable (with this particular setup) and not the lower limit.

It is also noteworthy that the heaviest coalescence tended to occur in the bottom half of the coalescence chamber. This indicates a 50 % reduction in residence time requirement. Furthermore, it is probable therefore that the chamber could have been as much as fifty percent shorter, without significantly decreasing the separator efficiency improvement. In fact, if the dust would have been withdrawn from the middle rather than from the top of the chamber, there is good reason to believe that the efficiency improvement would have been greater.

5.8 Scale-up Factor Analysis

Future scaleup potential requires that this method be capable of treating a sufficient volumetric flow in a small enough treatment volume. Table 5-5 shows a listing of current air cleaner systems ranked in order of cfm/air cleaner volume[13]. The new method should be of the same order of magnitude in order to fit into the existing space.

The cfm/coalescence chamber volume relationship for the tests conducted herein was in the range of 80 - 160 cfm per cubic foot. This range is based on results derived during the tests to determine the residence time. As noted above, these resident times represent the lowest residence times achieved-to-date, not the lower limit. At even lower residence times, the cfm/volume relationship goes up, hence the volume requirement decreases. Since these data are within the range of existing hardware, it is reasonable to believe that the ultrasonic coalescence method can fit into the available hardware envelope.

Table 5-5. Current Air Cleaner System Volumes

Vehicle	Ordnance No.	AirFlow	Dust Capacity	Volume	cfm/ft3
APU	13206E0250	80	1.9	0.4	200.00
M151	11681675	122	20	0.3	406.67
M551	11601345	350	7.6	0.69	507.25
M998	5584499	370	20	0.805	459.63
M35	10912376	410	2.9	0.84	488.10
M39	7737120	525	4	1.52	345.39
M809	11604557	550	20	2.32	237.07
M939	12256311	550	20	2.37	232.07
M125A1	10946144	565	6	1.09	518.35
M9ACE	12325739	610	30	2.02	301.98
M109A1	10914545	615	20	3.04	202.30
M113	10932291	700	3	1.34	522.39
M113A1	11598003	700	7.4	1.64	426.83
US M60	12251922	900	80	5.66	159.01
M60 Tank		900	200+	7.14	126.05
M2 IFV	12307204	980	28	3.96	247.47
LVTP7A1		1000	50	5.50	181.82
M915		1050	20	2.64	397.73
M88A1	11671216	1100	20	3.62	303.87
LAV-25	10501721	1190	26	3.06	388.89
HEM TT	1308990	1400	20	3.75	373.33
M1 Tank	12287727	10000	3.6	17.34	576.70
M1		10000	200+	17.96	556.79

LIST OF REFERENCES

1 Treuhaft, M. B., "Study of Fan-Airpump Applicability to Two-Stage Air Cleaner Systems, Final Report No. 13118, U. S. Army Contract No. DAAE07-84-C-R045, June 1985.

2 Treuhaft, M. B., "Agglomerating Self-Cleaning Air Cleaner", Final Report No. 13131, U. S. Army Contract No. DAAE07-83-C-R024, October 1985.

3 Gallego-Juarez, J. A., Rodriguez-Corral, G. and L. Gaete-Garreton, "An Ultrasonic Transducer for High Power Applications in Gases", Ultrasonics, p.267 (1978).

4 Taylor, S. R. and W. B. Tarpley, Jr., "Ultrasonic Coalescence for Scrubbing of Flue Gas Pollutants", Final Technical Report, U. S. Doe Contradt No. DE-AC02-81ER10974 (April 1983).

5 Taylor, S. R., "Ultrasonic Coalescence as Applied to Smoke Clearance of Shipboard Passageways", Final Report, U. S. Coast Guard Sponsorship (June 1983).

6 Taylor, C. M., Desai, P. M. and S. R. Taylor, "Enhanced Oil Recovery Process Water Cleanup via Ultrasonic Coalescence", Final Technical Report, U. S. Department of Energy Contract No. DE-AC01-86ER80346 (March 1987).

7 Brandt, O., et al.,"Zur Theorie der Akustischen Koagulation", Kolloid-Zeitschrift, 77, 103 (1936).

8 St. Clair, H. W., Industrial Engineering Chemistry, 41, 2434 (1949).

9 Tiwary, R. and G. Reethof, "Hydrodynamic Interaction of Spherical Aerosol Particles in a High Intensity Acoustic Field", J.Sound and Vibration, 108, 33 (1986).

10 Tiwary, R. and G. Reethof, "Numerical Simulation of Acoustic Agglomeration and Experimental Verification", J. Vibration, Stress and Reliability in Design, 109, 185 (1987).

11 George, W. and G. Reethof, "On the Fragility of Acoustically Agglomerated Submicron Fly Ash Particles", J. Vibration, Stress and Reliability in Design, 108, 322 (1986).

12 R. Tiwary, "Acoustic Agglomeration of Micron and Submicron Fly-ash Aerosols", Doctoral Thesis, Pennsylvania State University, May 1985.

13 H. R. Camplin, "Air Filtration System Design Principles", Final Technical Report, U. S. Army Contract No. DAAE07-83-C-R080, September 1985.

ADDENDUM

SEPARATION EFFICIENCY TEST DATA

Date	Test	Main	Scavnge	Freq	Pwr	Dust Conc	Eff'cy	Comment
Sep 10	A					10	11.4	4" tube
Sep 10	B					10	21	4" tube
Sep 10	C					10	45.7	4" tube
Sep 10	D					10	39	4" tube
Sep 10	E					10	63.3	4" tube
Sep 14	AU			27.3	25	10	65.2	Pos'n A
Sep 14	BU			27.3	25	10	67.7	Pos'n A
Sep 14	CU			27.3	25	10	68.6	Pos'n A
Sep 14	DU			27.3	25	10	62	Pos'n A
Sep 14	EU			27.3	25	10	56.0	Pos'n A
Sep 16	AUB			27.3	25	10	64.6	Pos'n B
Sep 16	BUB			27.3	25	10	58.9	Pos'n B
Sep 16	CUB			27.3	25	10	65.8	Pos'n B
Sep 16	DUB			27.3	25	10	61.7	Pos'n B
Sep 16	EUB			27.3	25	10	58.5	Pos'n B
Sep 24	A3/4					2	42.5	4" tube
Sep 24	B3/4					2	48.5	4" tube
Sep 24	C3/4					2	55	4" tube
Sep 24	D3/4					2	48	4" tube
Sep 24	A3/4U			27.1	25	2	47	4" tube
Sep 24	B3/4U			27.1	25	2	32.5	4" tube
Sep 24	C3/4U			27.1	25	2	40.5	4" tube
Sep 24	D3/4U			27.1	25	2	44	4" tube
Sep 24	E3/4			27.1	25	2	59.5	4" tube
Sep 28	A3/4UB			27.1	75	2	45	4" tube
Sep 28	B3/4UB			27.1	75	2	49	4" tube
Sep 28	C3/4UB			27.1	75	2	38.5	4" tube
Sep 28	D3/4UB			27.1	75	2	48.5	4" tube
Sep 28	E3/4UB			27.1	75	2	56	4" tube
Sep 29	A1/2					2	8.5	4" tube
Sep 29	B1/2					2	20	4" tube
Sep 29	C1/2					2	31	4" tube
Sep 29	D1/2					2	30	4" tube
Sep 29	A1/2U			27.1	25	2	10	4" tube
Sep 29	B1/2U			27.1	25	2	25.5	4" tube
Sep 29	C1/2U			27.1	25	2	41	4" tube
Sep 29	D1/2U			27.1	25	2	34.5	4" tube
Sep 29	E1/2U			27.1	25	2	33.5	4" tube
Sep 29	A1/2UB			27.1	75	2	42	4" tube
Sep 29	B1/2UB			27.1	75	2	35	4" tube
Sep 29	C1/2UB			27.1	75	2	40	4" tube
Sep 29	D1/2UB			27.1	75	2	42.5	4" tube
Sep 29	E1/2UB			27.1	75	2	37.5	4" tube
Oct 1	AF					2	55	4" tube
Oct 1	BF					2	56.5	4" tube

Date	Test	Main	Scavnge	Freq	Pwr	Dust Conc	Eff'cy	Comment
Oct 1	CF					2	63	4" tube
Oct 1	DF					2	56.5	4" tube
Oct 1	EF					2	58	4" tube
Oct 1	AF					10	74.7	4" tube
Oct 1	BF					10	82.8	4" tube
Oct 1	CF					10	71.4	4" tube
Oct 1	DF					10	76	4" tube
Oct 1	EF					10	72.9	4" tube
Oct 2	AFU			23.2	25	2	64.5	4" tube
Oct 2	BFU					2	68	4" tube
Oct 2	CFU					2	59.5	4" tube
Oct 2	DFU					2	54	4" tube
Oct 2	EFU					2	55.5	4" tube
Oct 2	AFU			23.2	25	10	73.5	4" tube
Oct 2	BFU			23.2	25	10	63	4" tube
Oct 2	CFU			23.2	25	10	72.2	4" tube
Oct 2	DFU			23.2	25	10	65.8	4" tube
Oct 2	EFU			23.2	25	10	66.6	4" tube
Oct 6	AFUB			23.2	75	2	37.5	4" tube
Oct 6	BFUB					2	50	4" tube
Oct 6	CFUB					2	53.5	4" tube
Oct 6	DFUB					2	60	4" tube
Oct 6	EFUB					2	55	4" tube
Oct 6	AFUB			23.2	75	10	69.5	4" tube
Oct 6	BFUB			23.2	75	10	72.3	4" tube
Oct 6	CFUB			23.2	75	10	60.9	4" tube
Oct 6	DFUB			23.2	75	10	62.1	4" tube
Oct 6	EFUB			23.2	75	10	60.8	4" tube
Oct 6	A1/2					10	43	4" tube
Oct 6	B1/2					10	32.5	4" tube
Oct 6	C1/2					10	29.7	4" tube
Oct 6	D1/2					10	24.2	4" tube
Oct 6	E1/2					10	50.7	4" tube
Oct 7	A1/2U			23.2	25	10	18.6	4" tube
Oct 7	B1/2U			23.2	25	10	19.3	4" tube
Oct 7	C1/2U			23.2	25	10	64.8	4" tube
Oct 7	D1/2U			23.2	25	10	37.8	4" tube
Oct 7	E1/2U			23.2	25	10	33.5	4" tube
Oct 7	A1/2UB			23.2	75	10	40.7	4" tube
Oct 7	B1/2UB			23.2	75	10	41.9	4" tube
Oct 7	C1/2UB			23.2	75	10	47.3	4" tube
Oct 7	D1/2UB			23.2	75	10	40.2	4" tube
Oct 7	E1/2UB			23.2	75	10	44.6	4" tube
Dec 4	1	111	11			N/D	N/D	
Dec 4	2	74	7.4			N/D	N/D	
Dec 4	3	47	4.7			N/D	N/D	
Dec 17	1	54.5	5.45			.00917;c	86.3%	
Dec 17	2	54.5	5.45			.00917;c	85.7%	
Dec 17	3	54.5	5.45			.00917;c	90.4%	

Date	Test	Main	Scavnge	Freq	Pwr	Dust Conc	Eff'cy	Comment
Dec 17	4	54.5	5.45			.00917;c	89.9%	
Dec 17	5	54.5	5.45			.00917;c	88.2%	
Dec 21	1	54.5	5.45			.00917;f	88.0%	
Dec 21	2	54.5	5.45			.00917;f	86.9%	
Dec 21	3	54.5	5.45			.00917;f	93.1%	
Dec 21	4	54.5	5.45			.00917;f	84.2%	
Dec 21	5	54.5	5.45			.00917;f	89.9%	
Dec 22	1	74	7.4			.0068;c	90.3%	
Dec 22	2	74	7.4			.0068;c	91.2%	
Dec 29	3	74	7.4			.0068;c	91.1%	
Dec 29	4	74	7.4			.0068;c	90.9%	
Dec 29	5	74	7.4			.0068;c	91.0%	
Jan 4	1	74	7.4			.0063;f	86.0%	
Jan 4	2	74	7.4			.0068;f	78%	
Jan 4	3	74	7.4			.0068	82%	
Jan 5	4	74	7.4			.0068;f	80%	
Jan 5	5	74	7.4			.0068;f	88%	
Jan 5	1	74	7.4	26.6	50	.0068;c	87%	
Jan 5	2	74	7.4	26.6	50	.0068;c	90%	
Jan 5	3	74	7.4	26.6	50	.0068;c	91%	
Jan 5	4	74	7.4	26.6	50	.0068;c	91.5%	
Jan 5	5	74	7.4	26.6	75	.0068;c	90.5%	
Jan 11	1	43	4.3			.045;c	93%	
Jan 11	2	43	4.3			.045;c	91%	
Jan 11	3	43	4.3			.093;c	92%	
Jan 11	4	43	4.3			.093;c	88%	
Jan 11	5	43	4.3			.093	90%	
Jan 11	1	43	4.3			.204;c	93%	
Jan 11	2	43	4.3			.204;c	92%	
Jan 11	3	43	4.3			.204;c	93%	
Jan 11	4	43	4.3			.204;c	90%	
Jan 12	5	43	4.3			.204;c	93%	
Jan 12	1	100;55	10;5.5			.108	91%	
Jan 12	2	100	10	20.7	80-90	.08	87%	
Jan 12	1	43	4.3	20.7	50	.18;c	90%	
Jan 12	2	43	4.3			.19;c	91%	
Jan 12	1	43	4.3			.194;f	86%	
Jan 12	2	43	4.3	20.5	50	.178;f	85%	
Jan 13	1	74;41	7.4			.161;f	85%	
Jan 13	2	69	6.9	20.6	100	.132;f	82%	
Jan 18	1	48	4.8			.025;f	81%	
Jan 18	2	64	6.4			.025;f	72%	
Jan 18	3	90	9.0			.025;f	71%	
Jan 18	1	88	8.8			.025;c	85%	
Jan 18	2	48	4.8			.025;c	90%	
Jan 18	3	48	4.8			.025;c	94%	
Jan 18	1	48	4.8	20.5	75	.025;c	84%	
Jan 18	2	74	7.4	20.5	75	.025;c	78%	
Jan 18	3	110	11	20.3	75	.025;c	76%	

Date	Test	Main	Scavnge	Freq	Pwr	Dust Conc	Eff'cy	Comment
Jan 18	1	100	10	20.4	75	.025;f	79%	
Jan 18	2	50	5.0	20.5	75	.025;f	85%	
Jan 18	3	43	4.3	20.3	75	.025;f	86%	
Jan 20	1	42	4.2			.20;f		
Jan 20	2	49	4.9	20.5	50-60	.17;f		

DISTRIBUTION LIST

	Copies
Commander Defense Technical Information Center Bldg. 5, Cameron Station ATTN: DDAC Alexandria, VA 22304-9990	12
Manager Defense Logistics Studies Information Exchange ATTN: AMXMC-D Fort Lee, VA 23801-6044	2
Commander U. S. Army Tank-Automotive Command ATTN: AMSTA-DDL (Technical Library) Warren, MI 48397-5000	2
Commander U. S. Army Tank-Automotive Command ATTN: AMSTA-RGT (Mr. J. Stevenson) Warren, MI 48397-5000	6
Commander U. S. Army Tank-Automotive Command ATTN: AMSTA-CF (Mr. G. Orlicki) Warren, MI 48397-5000	1
Director U.S. Army Materiel Systems Analysis Activity (AMSAA) ATTN: AMXSY-MP (Mr. Cohen) Aberdeen Proving Ground, MD 21005-5071	1